LysM-RLK plays an ancestral symbiotic function in plants

Eve Teyssier[1], Sabine Grat[1], Mélanie Rich[1], Pierre-Marc Delaux[1*], Malick Mbengue[1*]

[1] Laboratoire de Recherche en Sciences Végétales (LRSV), Université de Toulouse, CNRS, UPS, INP Toulouse, Castanet-Tolosan, France.

*Correspondence:
pierre-marc.delaux@cnrs.fr
malick.mbengue@univ-tlse3.fr

Highlights

- The LysM-RLK LYKa is essential for arbuscular mycorrhiza in *Marchantia paleacea*
- The only LYR from *Marchantia paleacea* is not required for arbuscular mycorrhiza
- LYKa and LYR are both required for chito- and lipochito-oligosaccharide signalling
- Lipochito- and chito-oligosaccharide signalling is not essential for arbuscular mycorrhiza in *Marchantia paleacea*

Summary

To ensure their water and mineral nutrition, most land plants form arbuscular mycorrhiza (AM) with soil-borne Glomeromycota fungi [1]. This ~450 million years old symbiosis was key in driving land colonisation by plants[2]. In angiosperms, AM is thought to be initiated via the perception by the host plant of AM-fungi derived chito- and lipochito-oligosaccharides leading to the activation of a conserved signalling pathway referred to as the Common Symbiosis Pathway[3]. Genetics in legumes and monocots have demonstrated that members of the Lysin motif Receptor-Like Kinase (LysM-RLK) family are important for the perception of these AM-fungi derived molecules, although none of the LysM-RLK mutants or combination of mutants described to date fully abolish AM[4]. This discrepancy with the phenotypes observed for components of the CSP, which fail to host AM fungi, might be the result of genetic redundancy between the multiple LysM-RLK paralogs found in these species. In contrast to angiosperms, the liverwort *Marchantia paleacea* contains only four LysM-RLKs. In this study, we demonstrate the essential role of one LysM-RLK for AM in *M. paleacea*. Furthermore, we present evidence that Marchantia's ability to respond to chito- or lipochito-oligosaccharides is not a predictor of its symbiotic ability, suggesting the existence of yet uncharacterized AM-fungi signals.

Results and Discussion

Phylogenetic analyses indicate that LysM-RLK originated in green algae and diversified following the colonisation of land by plants [5,6]. Extant liverworts harbour four clades, including three LYKs with a predicted active kinase and one LYR with a deleted activation loop in the kinase domain[7]. Based on the established nomenclature for LysM-RLKs[4], *M. paleacea* LYKa belongs to the LYK-I subclade that contains the immunity-related chitin co-receptor CERK1 from Arabidopsis[8] and the symbiotic Nod factor receptor NFR1 from *Lotus japonicus*[9] (Figure S1A). MpaLYKb and MpaLYKc are pro-orthologous to the LYK-II and LYK-III subclades while the single MpaLYR is pro-orthologous to the entire LYR-I to LYR-IV subclades (Figure S1A). *Marchantia polymorpha* that has lost the ability to form AM[10] contains two *LYKs* and one *LYR*[7]. Remnants in *M. polymorpha* of a third *LYK* gene, encoding a truncated receptor from the LYKb subclade, accounts for this discrepancy between Marchantia species (Figure S1A). All LysM-RLKs of *M. paleacea* contain a predicted N-terminal transit signal peptide, a LysMs-containing extracellular domain, a transmembrane region and an intracellular kinase. Transient expression in *Nicotiana benthamiana* and co-localization experiments with the Arabidopsis pattern-recognition receptor FLS2[11] confirmed a plasma membrane localisation for the four *M. paleacea* LysM-RLKs (Figure S1B).

Mutation of a single *LYK* gene in *Marchantia paleacea* leads to symbiosis impairment

To determine the contribution of individual LysM-RLKs from the *M. paleacea* LYK clade to arbuscular mycorrhiza, we generated loss-of-function mutants for *LYKa*, *LYKb* or *LYKc* using CRISPR/Cas9. Following plant transformations and subsequent progeny selection, we recovered independent mutant lines for each *LYK* gene. For *LYKa* and *LYKb*, only one guide-RNA led to frameshift-causing INDELs while the two different guide-RNAs designed against *LYKc* were effective in inducing *null* mutations (Figure S1C). We kept a minimum of two *null* mutant lines per receptor and treated them as different alleles due to their independent T-DNA insertions, irrespective of the causal *null* mutations. Next, we assessed the ability of the *lyk* mutants to form AM in comparison to an empty vector-containing control line. Six weeks after inoculation with spores of *Rhizophagus irregularis*, we evaluated the colonisation status of Marchantia by histological observations of transversal (Figure 1A) or longitudinal (Figure S2A) sections of the thallus. A strong pigmentation along the midrib of the thallus is a marker of a positive mycorrhizal colonisation in Marchantia[12]. This pigmentation is visible in control, *lykb* and *lykc* mutants but absent in *lyka*, suggesting successful symbiosis establishment in *lykb* and *lykc* and a lack of fungal colonisation in *lyka* (Figure 1A, S2A - middle panels). Wheat-Germ-Agglutinin (WGA)-Alexa Fluor staining of fungal membranes confirmed the presence of arbuscules-containing cells in the thalli of control, *lykb* and *lykc* plants. In contrast, no intercellular hyphae nor arbuscules-containing cells were labelled in *lyka* (Figure 1A, S2A – left and right panels), confirming the absence of AM formation in this mutant. Over two large scale experiments, quantitative analysis of the exclusion zone length[2] as well as the percentages of mycorrhizal plants per genotype did not reveal reproducible difference between *lykb* or *lykc* alleles versus control (Figure 1B, Figure S2B). These experiments

confirmed AM-defectiveness in all three *lyka* alleles tested, scoring approximately 300 thalli for this class of mutant in total (Figure 1B, Figure S2B). We therefore conclude that, within the *LYK* clade of *Marchantia paleacea*, *LYKa* is critical for AM establishment when *LYKb* and *LYKc* seem dispensable.

The absence of AM in *lyka* mirrors earlier AM-defective phenotypes observed in the rice *oscerk1* and *oscerk1/oscerk2* mutants, the two closest homologs of *LYKa* in that species[13,14]. However, those mutants still harboured arbuscules-containing cells albeit formed with a delay in comparison to control[13]. To verify that the absence of fungal colonisation in *lyka* was not due to a delay in AM establishment, we harvested *lyka* ten weeks after inoculation with *R. irregularis* spores. Again, we were unable to observe pigmentation or positive WGA-Alexa Fluor signal in the thalli of *lyka* plants inoculated under these conditions (Figure S2C). Thus, the absence of colonisation in *lyka* is not attributable to a delay in AM formation.

Mycorrhiza defects can be either the direct result of a missing signalling component in the host or the consequence of an indirect effect. For example, the lack of strigolactones (SLs) in the Marchantia biosynthetic mutant *Mpaccd8a/8b* severely compromises AM establishment due to a failure in initiating pre-symbiotic metabolic activity in the fungal partner[2]. Exogenous treatments with the synthetic SL-analogue GR24 efficiently complement symbiosis in *Mpaccd8a/8b*, demonstrating the indirect effect imposed by the *Mpaccd8a/8b* mutation on otherwise AM-capable plants[2]. Following that reasoning, we sought to test for trans-complementation of *lyka* when co-cultivated in proximity with wild-type Marchantia already hosting functional AM for several weeks. Six weeks after the start of the co-culture with nurse plants, empty-vector control plants displayed a ~86% success rate in fungal colonisation (Figure S2D). In contrast, none of the *lyka* plants grown under these conditions was colonised (Figure S2D). This suggests that the *lyka* phenotype is not due to a secondary effect on the fungal symbiont but is the direct consequence of a non-functioning LYKa-dependent signalling pathway in the host.

While angiosperm mutants in diverse LYKs showed delay or reduced colonisation rates[4,14–17], this work reports on a single LYK mutant displaying an AM phenotype no different from those observed for mutants of the CSP in angiosperms[18–25] or Marchantia (Vernié et al.). This supports the long-held hypothesis that perception of a fungal-derived molecule(s) by LysM-RLK is a prerequisite to AM establishment.

The single LYR gene from *Marchantia paleacea* is not essential for arbuscular mycorrhiza symbiosis

In angiosperms, the LYR subgroup has expanded, giving rise, for example, to five and ten paralogs in rice and *Medicago truncatula* respectively[4]. Because some of the *LYR* clades are phylogenetically linked with the AM symbiosis[26], the potential function of *LYRs* during AM symbiosis has been extensively studied. Single mutants have been tested for their symbiotic abilities in Medicago (*nfp* and *lyr4*)[27,28], Lotus (*Ljlys11*)[29], Parasponia (*Pannfp1, Pannfp2*)[17], tomato (*sllyk10*)[16], *Petunia (Phlyk10*)[16], barley (*rlk2* and *rlk10*)[21], and rice (*Osnfr5*)[30]. In addition, the double *nfp/lyr4 M. truncatula* mutant[27], *lys11/nfr5 L. japonicus* mutant[29], and the *rlk2/rlk10* barley mutant[21] were tested. Most of the single mutants displayed wild-type level of colonisation by AM fungi, with the exception of tomato and

Petunia single mutants, and even double mutants were either not or only partially affected in their AM fungi colonisation levels. The favoured hypothesis to explain these mixed results is the occurrence of significant genetic redundancy and variable contributions from the different paralogs in a species-specific manner.

Contrary to angiosperms, the genome of *M. paleacea* contains a single *LYR* gene[10] (Figure S1). To assess its contribution to symbiosis, we generated loss-of-function alleles using CRISPR/Cas9 (Figure S1B) and tested their ability to host AM. As previously performed for the *lyk* mutants, we evaluated the colonisation status of the *lyr* mutants by histological observations of transversal (Figure 2A) or longitudinal (Figure S3A) sections of the thallus. We observed no differences in thallus pigmentation between empty-vector control and *lyr*, suggesting similar colonisation levels in both genotypes. WGA-staining confirmed the presence of arbuscules in both control and *lyr* (Figure 2A, Figure S3A). Similarly to what we observed for the *lykb* and *lykc* mutants, quantitative analysis of the exclusion zone length[2] as well as the percentages of mycorrhizal plants per genotype did not point at reproducible differences between *lyr* alleles and control (Figure 1B, Figure S3B). Over two large scale experiments, control plants displayed a total of 98% mycorrhizal success rate, while the two *lyr* alleles followed closely with 92% and 96% mycorrhizal success rate. The mean lengths of the exclusion zone were similar between genotypes, although a slight difference of approx. 1mm was measured across replicates (Figure 2B, Figure S3B). The absence of mycorrhiza phenotype in mutants of the single *LYR* gene of *M. paleacea* demonstrates the non-essential role for this clade of LysM-RLK for AM symbiosis.

CO and LCO signalling is impaired in *lyka* and *lyr* mutants of *Marchantia paleacea*

Chito-oligosaccharides[31] (COs) and lipo-chitooligosaccharides[28] (LCOs) are two types of AM-derived chemical signals described to date. While some of the plant responses triggered by COs were considered immune- or symbiosis-specific depending on their degree of polymerization, recent studies challenged this view. Immune-associated compounds, such as peptidoglycan or large chitin fragment (CO8), can induce calcium spiking[27] in Medicago, while symbiosis-associated[31] short CO fragments (CO4) induce the transcription of defence-related genes[27,32]. To correlate AM establishment and perception of AM-derived signals, we sought to determine the signalling abilities of the different Marchantia LysM-RLK mutants in response to these compounds.

Ligands perception events by receptor-like kinases induce, within seconds, calcium influx into the cytosol and reactive oxygen species production in both immune and symbiotic contexts[33]. Here, we developed a Marchantia marker line for monitoring cytosolic calcium variations using a genetically encoded reporter. For that, we created a *M. paleacea* line expressing the cytosolic apoaequorin luminescent marker[34] under the control of the constitutive *MpoEF1α* promoter[35]. Once established and tested for suitable apoaequorin expression, this line served as an homogeneous background to create *de novo* all single *lyk* and *lyr* loss-of-function mutants using CRISPR/Cas9, as previously described (Figure S1B). A control line consisting of a transformant expressing the Cas9 endonuclease alone was also generated in the same genetic background (AEQ-cas9). Next, plants cultivated in AM permissive conditions were treated with commercially available chito-heptaose and chito-tetraose or a mixture of

fucosyl/methylfucosyl C18:1 LCOs, major forms of LCOs found in AM fungi[36]. Control plants responded to all three molecules applied at a final concentration of one micromolar (1µM) (Figure 3A). For all elicitor treatments, cytosolic free calcium concentration peaked 5 minutes after application before reaching back to the baseline at 15 minutes (Figure 3A). The maximum mean of free calcium concentration elicited by CO7 was the highest (1.2 µM), followed by CO4 (1µM) and LCOs (0.75µM) (Figure 3A). Importantly, dimethyl sulfoxide (DMSO) and water used to prepare stock solutions of CO7 or LCOs and CO4, respectively, did not trigger any calcium response in *M. paleacea* (Figure S4). Next, we tested the response of receptor mutants to CO7, CO4 and LCOs applied separately and at identical concentrations. The duration and amplitude of the calcium influxes obtained in AEQ-*lykb* and AEQ-*lykc* were similar to control for all three elicitors, while AEQ-*lyka* and AEQ-*lyr* failed to respond to all treatments (Figure 3B). Quantitative analyses of the area under the curves followed by ANOVA further confirmed the similarity between control, AEQ-*lykb* and AEQ-*lykc* and the statistical difference between control and AEQ-*lyka* or AEQ-*lyr* in response to CO7, CO4 or LCOs (Figure 3C). To rule out the possibility that *lyka* and *lyr* mutants generally fail to produce a calcium response, we treated all genotypes with hydrogen peroxide (H_2O_2) at a final concentration of 1mM. Like control, all four aequorin-expressing mutants responded to H_2O_2 with a strong calcium influx (Figure S5A). Quantitative analyses of the area under the curves followed by ANOVA confirmed the absence of difference between mutants and control after H_2O_2 treatment (Figure S5B). Altogether, this supports the conclusion that *lyka* and *lyr* are both required for perception of CO7, CO4 and LCOs in *M. paleacea*. These findings are in agreement with the report of *Marchantia polymorpha LYK1* and *LYR* being required for ROS production in response to CO7 and bacterial peptidoglycan[7].

For the last 10 years, short CO oligomers and LCOs have been presented as MYC-Factors, the blend of symbiotic signals produced by AM fungi to initiate symbiotic responses[28,31,37]. The fact that other compounds, such as CO8, can induce similar molecular and cellular first challenged this view[27]. In addition, large-scale analyses of exudates from sixty fungal species revealed that neither short COs nor LCOs are specific to AM fungi[36,38]. Our result supports a new hypothesis where the perception of currently-known MYC-factors is not essential for AM establishment (Figure 2 and 3B). From this, the existence of additional molecules, possibly specific to AM fungi, can be hypothesised. Such molecules would be perceived by a receptor independent of *Mpalyr* while their signalling would rely on *Mpalyka*. Future analyses of AM fungi exudates may allow identifying this signal in the future.

Conclusion

We demonstrate that mutating a single LysM-RLK in *M. paleacea* is sufficient to fully abolish AM, mirroring the phenotypes observed in mutants of the Common symbiosis pathway by Vernié *et al*. By contrast, abolishing the response to both COs and LCOs is not sufficient to reach the same phenotype, as observed in the *lyr* mutant. Our study reports the demonstration that the perception of symbiont-derived signals by LysM-RLK is essential for AM to occur, yet the nature of the signal(s) remains elusive. The suite of *Marchantia paleacea* mutants developed here offer the opportunity to identify these compounds in the future. The study of mutants in bryophyte species which have lost the

ability to form symbiosis allowed discovering the ancestral function of LysM-RLK in plant immunity[7,39]. Our work demonstrates that LysM-RLK have been maintained in land plant genomes for half a billion years with a dual function in immunity and symbiosis.

Acknowledgements

We would like to thank Vincent Garrigues, Manon Grousset, Lou Battaglia and Madeleine Baker for their technical assistance.

E.T. is supported by a PhD grant from the French Ministry of Higher Education and Research. Research performed at LRSV was supported by the 'Laboratoires d'Excellence (LABEX)' TULIP (ANR-10-LABX-41) and the 'École Universitaire de Recherche (EUR)' TULIP-GS (ANR-18-EURE-0019).

P-M.D is supported by the project Engineering Nitrogen Symbiosis for Africa (ENSA) funded through a grant to the University of Cambridge by the Bill and Melinda Gates Foundation (OPP1172165) and the UK Foreign, Commonwealth and Development Office as Engineering Nitrogen Symbiosis for Africa (OPP1172165) and by funding from the European Research Council (ERC) under the European Union's Horizon 2020 research and innovation programme (grant agreement no. 101001675 - ORIGINS) to P.-M.D.

Author contributions

E.T. and M.M. designed and coordinated the experiments. E.T., S.G., M.R. and M.M. conducted experiments. E.T., P.M.D. and M.M. wrote the manuscript. M.M. coordinated the project.

References

1. Smith, S.E., and Read, D.J. (2002). Mycorrhizal symbiosis (Elsevier) 10.1016/B978-0-12-652840-4.X5000-1.

2. Kodama, K., Rich, M.K., Yoda, A., Shimazaki, S., Xie, X., Akiyama, K., Mizuno, Y., Komatsu, A., Luo, Y., Suzuki, H., et al. (2022). An ancestral function of strigolactones as symbiotic rhizosphere signals. Nat Commun *13*, 3974. 10.1038/s41467-022-31708-3.

3. Kistner, C., and Parniske, M. (2002). Evolution of signal transduction in intracellular symbiosis. Trends in Plant Science *7*, 511–518. 10.1016/S1360-1385(02)02356-7.

4. Buendia, L., Girardin, A., Wang, T., Cottret, L., and Lefebvre, B. (2018). LysM Receptor-Like Kinase and LysM Receptor-Like Protein families: An update on phylogeny and functional characterization. Front. Plant Sci. *9*, 1531. 10.3389/fpls.2018.01531.

5. Delaux, P.-M., Radhakrishnan, G.V., Jayaraman, D., Cheema, J., Malbreil, M., Volkening, J.D., Sekimoto, H., Nishiyama, T., Melkonian, M., Pokorny, L., et al. (2015). Algal ancestor of land plants was preadapted for symbiosis. Proc. Natl. Acad. Sci. U.S.A. *112*, 13390–13395. 10.1073/pnas.1515426112.

6. Nishiyama, T., Sakayama, H., De Vries, J., Buschmann, H., Saint-Marcoux, D., Ullrich, K.K., Haas, F.B., Vanderstraeten, L., Becker, D., Lang, D., et al. (2018). The Chara genome: Secondary complexity and implications for plant terrestrialization. Cell *174*, 448-464.e24. 10.1016/j.cell.2018.06.033.

7. Yotsui, I., Matsui, H., Miyauchi, S., Iwakawa, H., Melkonian, K., Schlüter, T., Michavila, S., Kanazawa, T., Nomura, Y., Stolze, S.C., et al. (2023). LysM-mediated signaling in *Marchantia polymorph* highlights the

conservation of pattern-triggered immunity in land plants. Current Biology *33*, 3732-3746.e8. 10.1016/j.cub.2023.07.068.

8. Miya, A., Albert, P., Shinya, T., Desaki, Y., Ichimura, K., Shirasu, K., Narusaka, Y., Kawakami, N., Kaku, H., and Shibuya, N. (2007). CERK1, a LysM receptor kinase, is essential for chitin elicitor signaling in *Arabidopsis*. Proc. Natl. Acad. Sci. U.S.A. *104*, 19613–19618. 10.1073/pnas.0705147104.

9. Radutoiu, S., Madsen, L.H., Madsen, E.B., Felle, H.H., Umehara, Y., Grønlund, M., Sato, S., Nakamura, Y., Tabata, S., Sandal, N., et al. (2003). Plant recognition of symbiotic bacteria requires two LysM receptor-like kinases. Nature *425*, 585–592. 10.1038/nature02039.

10. Radhakrishnan, G.V., Keller, J., Rich, M.K., Vernié, T., Mbadinga Mbadinga, D.L., Vigneron, N., Cottret, L., Clemente, H.S., Libourel, C., Cheema, J., et al. (2020). An ancestral signalling pathway is conserved in intracellular symbioses-forming plant lineages. Nat. Plants *6*, 280–289. 10.1038/s41477-020-0613-7.

11. Robatzek, S., Chinchilla, D., and Boller, T. (2006). Ligand-induced endocytosis of the pattern recognition receptor FLS2 in *Arabidopsis*. Genes Dev. *20*, 537–542. 10.1101/gad.366506.

12. Humphreys, C.P., Franks, P.J., Rees, M., Bidartondo, M.I., Leake, J.R., and Beerling, D.J. (2010). Mutualistic mycorrhiza-like symbiosis in the most ancient group of land plants. Nat Commun *1*, 103. 10.1038/ncomms1105.

13. Miyata, K., Kozaki, T., Kouzai, Y., Ozawa, K., Ishii, K., Asamizu, E., Okabe, Y., Umehara, Y., Miyamoto, A., Kobae, Y., et al. (2014). The bifunctional plant receptor, OsCERK1, regulates both chitin-triggered immunity and arbuscular mycorrhizal symbiosis in Rice. Plant and Cell Physiology *55*, 1864–1872. 10.1093/pcp/pcu129.

14. Miyata, K., Hasegawa, S., Nakajima, E., Nishizawa, Y., Kamiya, K., Yokogawa, H., Shirasaka, S., Maruyama, S., Shibuya, N., and Kaku, H. (2022). OsCERK2/OsRLK10, a homolog of OsCERK1, has a potential role for chitin-triggered immunity and arbuscular mycorrhizal symbiosis in rice. Plant Biotechnology *39*, 119–128. 10.5511/plantbiotechnology.21.1222a.

15. Gibelin-Viala, C., Amblard, E., Puech-Pages, V., Bonhomme, M., Garcia, M., Bascaules-Bedin, A., Fliegmann, J., Wen, J., Mysore, K.S., Le Signor, C., et al. (2019). The *Medicago truncatula* LysM receptor-like kinase LYK9 plays a dual role in immunity and the arbuscular mycorrhizal symbiosis. New Phytologist *223*, 1516–1529. 10.1111/nph.15891.

16. Girardin, A., Wang, T., Ding, Y., Keller, J., Buendia, L., Gaston, M., Ribeyre, C., Gasciolli, V., Auriac, M.-C., Vernié, T., et al. (2019). LCO receptors involved in arbuscular mycorrhiza are functional for rhizobia perception in legumes. Current Biology *29*, 4249-4259.e5. 10.1016/j.cub.2019.11.038.

17. Rutten, L., Miyata, K., Roswanjaya, Y.P., Huisman, R., Bu, F., Hartog, M., Linders, S., Van Velzen, R., Van Zeijl, A., Bisseling, T., et al. (2020). Duplication of symbiotic lysin motif receptors predates the evolution of nitrogen-fixing nodule symbiosis. Plant Physiol. *184*, 1004–1023. 10.1104/pp.19.01420.

18. Stracke, S., Kistner, C., Yoshida, S., Mulder, L., Sato, S., Kaneko, T., Tabata, S., Sandal, N., Stougaard, J., Szczyglowski, K., et al. (2002). A plant receptor-like kinase required for both bacterial and fungal symbiosis. Nature *417*, 959–962. 10.1038/nature00841.

19. Endre, G., Kereszt, A., Kevei, Z., Mihacea, S., Kaló, P., and Kiss, G.B. (2002). A receptor kinase gene regulating symbiotic nodule development. Nature *417*, 962–966. 10.1038/nature00842.

20. Gutjahr, C., Banba, M., Croset, V., An, K., Miyao, A., An, G., Hirochika, H., Imaizumi-Anraku, H., and Paszkowski, U. (2008). Arbuscular mycorrhiza–specific signaling in rice transcends the common symbiosis signaling pathway. The Plant Cell *20*, 2989–3005. 10.1105/tpc.108.062414.

21. Li, X.-R., Sun, J., Albinsky, D., Zarrabian, D., Hull, R., Lee, T., Jarratt-Barnham, E., Chiu, C.H., Jacobsen, A., Soumpourou, E., et al. (2022). Nutrient regulation of lipochitooligosaccharide recognition in plants via NSP1 and NSP2. Nat Commun *13*, 6421. 10.1038/s41467-022-33908-3.

22. Yano, K., Yoshida, S., Müller, J., Singh, S., Banba, M., Vickers, K., Markmann, K., White, C., Schuller, B., Sato, S., et al. (2008). CYCLOPS, a mediator of symbiotic intracellular accommodation. Proc. Natl. Acad. Sci. U.S.A. *105*, 20540–20545. 10.1073/pnas.0806858105.

23. Messinese, E., Mun, J.-H., Yeun, L.H., Jayaraman, D., Rougé, P., Barre, A., Lougnon, G., Schornack, S., Bono, J.-J., Cook, D.R., et al. (2007). A novel nuclear protein interacts with the symbiotic DMI3 calcium- and calmodulin-dependent protein kinase of *Medicago truncatula*. MPMI *20*, 912–921. 10.1094/MPMI-20-8-0912.

24. Lévy, J., Bres, C., Geurts, R., Chalhoub, B., Kulikova, O., Duc, G., Journet, E.-P., Ané, J.-M., Lauber, E., Bisseling, T., et al. (2004). A putative Ca^{2+} and calmodulin-dependent protein kinase required for bacterial and fungal symbioses. Science *303*, 1361–1364. 10.1126/science.1093038.

25. Catoira, R., Galera, C., de Billy, F., Penmetsa, R.V., Journet, E.-P., Maillet, F., Rosenberg, C., Cook, D., Gough, C., and Dénarié, J. Four genes of *Medicago truncatula* controlling components of a nod factor ttransduction pathway.

26. Delaux, P.-M., Varala, K., Edger, P.P., Coruzzi, G.M., Pires, J.C., and Ané, J.-M. (2014). Comparative phylogenomics uncovers the impact of symbiotic associations on host genome evolution. PLoS Genet *10*, e1004487. 10.1371/journal.pgen.1004487.

27. Feng, F., Sun, J., Radhakrishnan, G.V., Lee, T., Bozsóki, Z., Fort, S., Gavrin, A., Gysel, K., Thygesen, M.B., Andersen, K.R., et al. (2019). A combination of chitooligosaccharide and lipochitooligosaccharide recognition promotes arbuscular mycorrhizal associations in Medicago truncatula. Nat Commun *10*, 5047. 10.1038/s41467-019-12999-5.

28. Maillet, F., Poinsot, V., André, O., Puech-Pagès, V., Haouy, A., Gueunier, M., Cromer, L., Giraudet, D., Formey, D., Niebel, A., et al. (2011). Fungal lipochitooligosaccharide symbiotic signals in arbuscular mycorrhiza. Nature *469*, 58–63. 10.1038/nature09622.

29. Rasmussen, S.R., Füchtbauer, W., Novero, M., Volpe, V., Malkov, N., Genre, A., Bonfante, P., Stougaard, J., and Radutoiu, S. (2016). Intraradical colonization by arbuscular mycorrhizal fungi triggers induction of a lipochitooligosaccharide receptor. Sci Rep *6*, 29733. 10.1038/srep29733.

30. Miyata, K., Hayafune, M., Kobae, Y., Kaku, H., Nishizawa, Y., Masuda, Y., Shibuya, N., and Nakagawa, T. (2016). Evaluation of the role of the LysM Receptor-Like Kinase, OsNFR5/OsRLK2 for AM symbiosis in Rice. Plant Cell Physiol *57*, 2283–2290. 10.1093/pcp/pcw144.

31. Genre, A., Chabaud, M., Balzergue, C., Puech-Pagès, V., Novero, M., Rey, T., Fournier, J., Rochange, S., Bécard, G., Bonfante, P., et al. (2013). Short-chain chitin oligomers from arbuscular mycorrhizal fungi trigger nuclear Ca^{2+} spiking in *Medicago truncatula* roots and their production is enhanced by strigolactone. New Phytologist *198*, 190–202. 10.1111/nph.12146.

32. Bozsoki, Z., Cheng, J., Feng, F., Gysel, K., Vinther, M., Andersen, K.R., Oldroyd, G., Blaise, M., Radutoiu, S., and Stougaard, J. (2017). Receptor-mediated chitin perception in legume roots is functionally separable from Nod factor perception. Proc. Natl. Acad. Sci. U.S.A. *114*. 10.1073/pnas.1706795114.

33. Zipfel, C., and Oldroyd, G.E.D. (2017). Plant signalling in symbiosis and immunity. Nature *543*, 328–336. 10.1038/nature22009.

34. Knight, M.R., Read, N.D., Campbell, A.K., and Trewavas, A.J. (1993). Imaging calcium dynamics in living plants using semi-synthetic recombinant aequorins. The Journal of Cell Biology *121*.

35. Althoff, F., Kopischke, S., Zobell, O., Ide, K., Ishizaki, K., Kohchi, T., and Zachgo, S. (2014). Comparison of the MpEF1α and CaMV35 promoters for application in *Marchantia polymorpha* overexpression studies. Transgenic Res *23*, 235–244. 10.1007/s11248-013-9746-z.

36. Rush, T.A., Puech-Pagès, V., Bascaules, A., Jargeat, P., Maillet, F., Haouy, A., Maës, A.Q., Carriel, C.C., Khokhani, D., Keller-Pearson, M., et al. (2020). Lipo-chitooligosaccharides as regulatory signals of fungal growth and development. Nat Commun *11*, 3897. 10.1038/s41467-020-17615-5.

37. Genre, A., Lanfranco, L., Perotto, S., and Bonfante, P. (2020). Unique and common traits in mycorrhizal symbioses. Nat Rev Microbiol *18*, 649–660. 10.1038/s41579-020-0402-3.

38. Cope, K.R., Bascaules, A., Irving, T.B., Venkateshwaran, M., Maeda, J., Garcia, K., Rush, T.A., Ma, C., Labbé, J., Jawdy, S., et al. (2019). The ectomycorrhizal fungus *Laccaria bicolor* produces lipochitooligosaccharides and uses the common symbiosis pathway to colonize *Populus* roots. Plant Cell *31*, 2386–2410. 10.1105/tpc.18.00676.

39. Bressendorff, S., Azevedo, R., Kenchappa, C.S., Ponce De León, I., Olsen, J.V., Rasmussen, M.W., Erbs, G., Newman, M.-A., Petersen, M., and Mundy, J. (2016). An innate immunity pathway in the moss *Physcomitrella patens*. The Plant Cell *28*, 1328–1342. 10.1105/tpc.15.00774.

40. Balzergue, C., Puech-Pagès, V., Bécard, G., and Rochange, S.F. (2011). The regulation of arbuscular mycorrhizal symbiosis by phosphate in pea involves early and systemic signalling events. Journal of Experimental Botany *62*, 1049–1060. 10.1093/jxb/erq335.

41. Kelly, S., Hansen, S.B., Rübsam, H., Saake, P., Pedersen, E.B., Gysel, K., Madland, E., Wu, S., Wawra, S., Reid, D., et al. (2023). A glycan receptor kinase facilitates intracellular accommodation of arbuscular mycorrhiza and symbiotic rhizobia in the legume Lotus japonicus. PLoS Biol *21*, e3002127. 10.1371/journal.pbio.3002127.

42. Kalyaanamoorthy, S., Minh, B.Q., Wong, T.K.F., von Haeseler, A., and Jermiin, L.S. (2017). ModelFinder: fast model selection for accurate phylogenetic estimates. Nat Methods *14*, 587–589. 10.1038/nmeth.4285.

43. Nguyen, L.-T., Schmidt, H.A., Von Haeseler, A., and Minh, B.Q. (2015). IQ-TREE: A fast and effective stochastic algorithm for estimating maximum-likelihood phylogenies. Molecular Biology and Evolution *32*, 268–274. 10.1093/molbev/msu300.

44. Hoang, D.T., Chernomor, O., Von Haeseler, A., Minh, B.Q., and Vinh, L.S. (2018). UFBoot2: Improving the Ultrafast Bootstrap Approximation. Molecular Biology and Evolution *35*, 518–522. 10.1093/molbev/msx281.

45. Letunic, I., and Bork, P. (2021). Interactive Tree Of Life (iTOL) v5: an online tool for phylogenetic tree display and annotation. Nucleic Acids Research *49*, W293–W296. 10.1093/nar/gkab301.

46. Schiessl, K., Lilley, J.L.S., Lee, T., Tamvakis, I., Kohlen, W., Bailey, P.C., Thomas, A., Luptak, J., Ramakrishnan, K., Carpenter, M.D., et al. (2019). NODULE INCEPTION recruits the lateral root developmental program for symbiotic nodule organogenesis in *Medicago truncatula*. Current Biology *29*, 3657-3668.e5. 10.1016/j.cub.2019.09.005.

47. Li, J.-F., Norville, J.E., Aach, J., McCormack, M., Zhang, D., Bush, J., Church, G.M., and Sheen, J. (2013). Multiplex and homologous recombination–mediated genome editing in Arabidopsis and Nicotiana benthamiana using guide RNA and Cas9. Nat Biotechnol *31*, 688–691. 10.1038/nbt.2654.

48. Brini, M., Marsault, R., Bastianutto, C., Alvarez, J., Pozzan, T., and Rizzuto, R. (1995). Transfected aequorin in the measurement of cytosolic Ca2+ concentration. Journal of Biological Chemistry *270*, 9896–9903. 10.1074/jbc.270.17.9896.

LEAD CONTACT AND MATERIALS AVAILABILITY

Further information and requests for resources and reagents should be directed to and will be fulfilled by the Lead Contact, Malick Mbengue (malick.mbengue@univ-tlse3.fr).

EXPERIMENTAL MODEL AND SUBJECT DETAILS

Plant material, growth conditions and transformation

Plant transformation

Marchantia paleacea ssp paleacea wild-type plants were grown axenically *in vitro* from sterile gemmae on ½ strength Gamborg B5 (G5768, Sigma) medium supplemented with 1.4 % agar (1330, Euromedex) for 4 to 5 weeks in 16/8h photoperiod at 22°C/20°C. For transformation, ~20 plantlets were blended 15

seconds in a sterile 250ml stainless steel bowl (Waring, USA) in 10mL of OM51C medium [KNO_3 (2 $g.L^{-1}$), NH_4NO_3 (0.4 $g.L^{-1}$), $MgSO_4$ $7H_2O$ (0.37 $g.L^{-1}$), $CaCl_2$ $2H_2O$ (0.3 $g.L^{-1}$), KH_2PO_4 (0.275 $g.L^{-1}$), L-glutamine (0.3 $g.L^{-1}$), casamino-acids (1 $g.L^{-1}$), Na_2MoO_4 2H2O (0.25 $mg.L^{-1}$), $CuSO_4$ $5H_2O$ (0.025 $mg.L^{-1}$), $CoCl_2$ $6H_2O$ (0.025 $mg.L^{-1}$), $ZnSO_4$ 7H2O (2 $mg.L^{-1}$), $MnSO_4$ H2O (10 $mg.L^{-1}$), H_3BO_3 (3 $mg.L^{-1}$), KI (0.75$mg.L^{-1}$), EDTA ferric sodium (36.7 $mg.L^{-1}$), myo-inositol (100 $mg.L^{-1}$), nicotinic acid (1 $mg.L^{-1}$), pyridoxine HCL (1 $mg.L^{-1}$), thiamine HCL (10$mg.L^{-1}$)]. The blended plant tissues were transferred to 250ml erlenmeyers containing 150ml of OM51C and kept at 22°C/20°C, 16/8h photoperiod, 200 RPM for 3 days. Co-cultures with *A. tumefaciens* (GV3101) containing constructs were initiated by adding 100µL of saturated bacterial liquid culture and acetosyringone (100 µM final). After 3 days, plant fragments were washed by decantation 3 times with water and plated on ½ Gamborg containing 200 $mg.L^{-1}$ amoxicillin (Levmentin, Laboratoires Delbert, FR) and 10 $mg.L^{-1}$ Hygromycin or 50nM Chlorsulfuron (34322-100MG Sigma).

Biological assays

For AM experiments, *Marchantia paleacea ssp paleacea* control and mutants were grown on a zeolite substrate (50% fraction 1.0-2,5mm, 50% fraction 0,5-1.0-mm, Symbiom) in 7x7x8 cm pots with a density of five thalli per pot. Pots were watered once a week with Long Ashton medium containing 7.5 µM of phosphate[40] and grown with a 16/8h photoperiod at 22°C/20°C for at least 2 weeks prior inoculation with AM fungi. For calcium measurement, similar conditions were applied with the exception of a higher plant density per pot and a growth duration of 4 weeks.

Phylogeny

To reconstruct the phylogeny of LysM-RLKs, a set of 102 protein sequences composed of 8 Marchantia genes and the set described by Buendia et al. (2018) supplemented with the *Lotus japonicus* EPR3a sequence[41] was aligned using MUSCLE (v3.8). The phylogeny was reconstructed using IQ-TREE v1.6.12 (http://iqtree.cibiv.univie.ac.at/) with the VT+F+I+G4 model and support was provided with 1,000 ultrafast bootstrap replicates[42–44]. The unrooted tree visualisation was generated using iTOL[45].

Cloning

The Golden Gate modular cloning system was used to prepare the plasmids as described in *Schiessl et al*[46]. Level 1 and Level 2 empty vectors used in this study are listed in the Key Resources Table and held for distribution in the ENSA project core collection (https://www.ensa.ac.uk/). Other Level 0, Level 1 and Level 2 vectors containing constructs are listed in the Key Resources Table. Coding sequences were either domesticated in-house in the pUPD2 vector or synthesised and cloned into pMS (GeneArt, Thermo Fisher Scientific, Waltham, USA).

Transient expression assays in *Nicotiana benthamiana*

Agrobacterium tumefaciens (GV3101) cultures carrying vectors of interest (see key resources table) were grown under agitation overnight at 28°C in liquid LB medium supplemented with adequate antibiotics. Cultures were washed twice by centrifugation at 8000g and resuspended in water supplemented with 50 µM acetosyringone. Bacteria concentrations were adjusted to OD_{600}=0.2 per construct prior infiltration of the abaxial side of two months old *N. benthamiana* leaves using 1 mL needleless syringe. After 48 hrs, mCherry and GFP signals were sequentially acquired using a Leica SP8 confocal microscope mounted with a FLUOTAR VISIR 25x/0.95NA water immersion objective (Leica). GFP was excited at 488 nm and detected from 500 to 535 nm. Monomeric Cherry was excited at 552 nm and detected from 560 to 610 nm.

Generation of CRISPR mutants in *M. paleacea ssp. paleacea*

Constructs containing the *A. thaliana* codon-optimised SpCas9[47] under the *MpoEF1α* promoter and single guide RNAs (Table Suppl. 1) under the *M. polymorpha* U6 promoter were transformed in *M. paleacea.* Two alleles of *lyka, lykb, lykc* and *lyr* were selected for AM phenotyping. A *M. paleacea* line expressing the calcium reporter aequorin under the *MpoEF1α* promoter was retransformed with the CRISPR/Cas9 vectors modified to contain a secondary selection marker. One line per AEQ/mutant was used for calcium assays.

Mycorrhization tests

Each pot was inoculated with ~1,000 sterile spores of *Rhizophagus irregularis* DAOM 197198 (Agronutrition, Labège, France). For the nursing experiment, thalli of empty-vector control and *lyka* were transplanted in proximity to wild-type plants inoculated with *R. irregularis* spores more than 10 weeks before. Six or ten weeks post-inoculation (or nursing), thalli were cleared of chlorophyll using ethanol 100% for 1 day before storage in an EDTA (0.5 mM). Cleared thalli were scanned with an EPSON 11000XL and the distance between apical notches and the colonisation zone (naturally coloured with a purple/brown pigment) were scored on using ImageJ. Large-scale mycorrhization assays were run independently twice.

For imaging, cleared thalli of control and of one mutant allele per receptor were embedded in 6% agarose and 100 µm thick transversal and longitudinal sections were prepared using a Leica VT1000s vibratome. Sections were incubated overnight in 10% K-OH (w/v) prior to three washes in PBS. Pictures were taken with a Zeiss AxioZoom V16 binocular using a PlanApo Z 0.5X.objective and the ZEN software suite with similar settings. Fungal membranes were stained overnight using 1 $\mu g.mL^{-1}$ WGA-Alexa Fluor 488 (Sigma) diluted in PBS. Alexa Fluor was excited between 450 and 490 nm and emission collected between 500 and 550 nm.

Calcium influx measurements

Four weeks old plants grown in low phosphate conditions were submerged in 2.5 µM coelenterazine-h (Interchim) diluted in water for a minimum of 16 hrs at room temperature in the dark. Samples were then transferred in a Berthold Sirius luminometer before treatments with a 250 µL aqueous solution of

1 µM CO7, 1 µM CO4 (Elicityl, Crolles, France) or a 1 µM mixture of fucosyl/methylfucosyl C18:1 LCOs (gift from Pr. Guillaume Becard). Luminescence was continuously recorded for 15 min using a 1 sec interval. An equal volume of 2X lysis buffer [20% ETOH, 10mM CaCl2 , 2% NP-40] was injected to discharge the total luminescence left and light was collected for an additional 5 min. Calcium concentrations were calibrated as previously done[48]. Graphs were prepared using RStudio and the ggplot2 package by plotting signals from 10 to 900 seconds after treatment. Areas under the curve were calculated by addition of calcium concentrations minus baselines, defined by the lowest value in each trace.

Statistical analyses and graphs

ANOVA were performed using GraphPad (www.graphpad.com). Dunn's multiple comparison test and Dunnet's multiple comparison test were applied to evaluate differences versus control, for phenotypic characterisation and calcium measurements, respectively. Only significant differences versus control are reported.

FIGURE LEGENDS

Figure 1. *LYKa* is essential for arbuscular mycorrhizal symbiosis in *M. paleacea*.

(**A**) Transversal sections of *M. paleacea* control (E.V.) or single *lyka-1* mutants six weeks after inoculation with *Rhizophagus irregularis*. Left panels are overlays of bright fields (middle panels) and fluorescent images (right panels) of wheat germ agglutinin (WGA) coupled to Alexa Fluor 488 to detect fungal structures. Dashed line-delimited insets are enlarged underneath the original images. Scale bars are 500µm and 200µm for insets.

(**B**) Exclusion zone length on mycorrhized plants for control (E.V.) and loss-of-function *lyk* mutants. Fractions in bold grey represent mycorrhized thalli over total thalli assessed for each genotype. Adjusted p-values for Dunn's multiple comparisons test versus control are shown (**<0.01). Control (E.V.) values are shared with figure 2.

Figure 2. *LYR* is dispensable for arbuscular mycorrhizal symbiosis in *M. paleacea*.

(**A**) Transversal sections of *M. paleacea* control (E.V.) or the *lyr-2* mutant six weeks after inoculation with *Rhizophagus irregularis*. Left panels are overlays of bright field (middle panels) and fluorescent images (right panels) of wheat germ agglutinin (WGA) coupled to Alexa Fluor 488 (FITC) to detect fungal structures. Dashed line-delimited insets are enlarged underneath the original images. Scale bars are 500 µm and 200 µm for insets.

(**B**) Exclusion zone length on mycorrhized plants for control (E.V.) or two independent *lyr* mutants. For each genotype, fractions in bold grey represent mycorrhized thalli over total thalli assessed. Control values are shared with figure 1.

Figure 3. LYKa and LYR are essential for chitooligosaccharides- and lipochitooligosaccharide-induced cytosolic calcium influx in *M. paleacea*.

(**A**) Cytosolic calcium influx in *M. paleacea* control (AEQ-cas9) or (**B**) single *lysm-rlk* mutants (as indicated) treated with 1µM chitoheptaose (CO7– left column), 1 µM chitotetraose (CO4 – middle column) or 1µM LCOs (right column). Each trace represents the mean (line) ± standard deviation (shading) from at least three replicates over a time course of 15 min.

(**C**) Bar graph representation of the area under the curves (A.U.C.) shown in (A). p-values for Dunnett's multiple comparisons test versus control are shown (* < 0,05; ** < 0,01; *** < 0,001; **** <0,0001).

Suppl. Figure 1. *Marchantia paleacea* possesses four LysM Receptor-Like Kinases.

(**A**) Phylogenetic analysis of LysM-RLKs from land plant species. Full-length protein sequences from *A. thaliana* (AT), *S. lycopersicum* (Solyc), *O. sativa* (Os), *P. persica* (Prupe), *L. japonicus* (Lj), *M. truncatula* (Medtr), *M. polymorpha* (Mapoly) and *M. paleacea* (Marpal) were aligned with MUSCLE prior unrooted Maximum Likelihood phylogenetic tree construction using a 1000 bootstraps resampling value. Branch colours indicate bootstrap values. Four phylogenetic sub-groups are highlighted: LYK-A (blue), LYK-B (orange), LYK-C (green), LYR (pink). *M. paleacea* proteins are labelled in red. The star sign indicates the truncated LYKb homolog in *M. polymorpha*. Notable receptors for chitin perception in Arabidopsis and Nod factors perception in legumes are annotated with yellow and green dots, respectively.

(**B**) Confocal micrographs of *Nicotiana benthamiana* epidermal cells transiently co-expressing *M. paleacea* LysM-RLKs-mCherry fusions (left panel - as indicated) and the plasma membrane marker AtFLS2-GFP (middle panel). Overlays including bright fields are shown. Scale bars = 25 µm.

(**C**) Schematic representation of *M. paleacea LysM-RLKs* gene structure: exons (grey boxes), introns (black line), transmembrane domain coding sequence (green boxes). Arrows point at guide RNAs positions used for generating CRISPR/Cas9 loss-of-function mutants.

Suppl. Figure 2. *LYKa* is essential for arbuscular mycorrhizal symbiosis in *M. paleacea*.

(**A**) Longitudinal sections of *M. paleacea* control (E.V.) or single *lyka-1* mutants six weeks after inoculation with *Rhizophagus irregularis*.

(**B**) Exclusion zone length on mycorrhized plants for control (E.V.) and loss-of-function *lyk* mutants. For each genotype, fractions in bold grey represent mycorrhized thalli over total thalli assessed. Control values are shared with supplemental figure 3.

(**C**) Longitudinal sections of the *lyka-1* mutant 10 weeks after inoculation with *Rhizophagus irregularis*.

(**D**) Longitudinal sections of *M. paleacea* control (E.V.) or the *lyka-1* mutant six weeks after co-cultivation with mycorrhized *M. paleacea* nurse plants. Fractions in black represent mycorrhized thalli over total thalli assessed. Scale bar = 200 µm.

(**A, C, D**) Left panels are overlays of bright field (middle panels) and fluorescent images (right panels) of wheat germ agglutinin (WGA) coupled to Alexa Fluor 488 to detect fungal structures.

(**A, C**) Dashed line-delimited insets are enlarged underneath the original images. Scale bars are 500 µm and 200 µm for insets.

Suppl. Figure 3. *LYR* is dispensable for arbuscular mycorrhizal symbiosis in *M. paleacea*.

(**A**) Longitudinal sections of *M. paleacea* control (E.V.) or the *lyr-2* mutants six weeks after inoculation with *Rhizophagus irregularis*. Left panels are overlays of bright field (middle panels) and fluorescent images (right panels) of wheat germ agglutinin (WGA) coupled to Alexa Fluor 488 to detect fungal structures. Dashed line-delimited insets are enlarged underneath the original images. Scale bars are 500 µm and 200 µm for insets.

(**B**) Exclusion zone length on mycorrhized plants for control (E.V.) and two independent *lyr* mutants. For each genotype, fractions in bold grey represent mycorrhized thalli over total thalli assessed. Adjusted p-values for Dunn's multiple comparisons test versus control are shown (**<0.01). Control values are shared with supplemental figure 2.

Suppl. Figure 4. Carriers do not elicit calcium influx in *M. paleacea.*

Cytosolic calcium influx in *M. paleacea* control plants (AEQ-cas9) in response to (**A**) 0.1% DMSO diluted in water or (**B**) water, over a time course of 15 min.

Suppl. Figure 5. *M. paleacea* LysM-RLKs mutants produce a calcium influx in response to hydrogen peroxide.

(**A**) Cytosolic calcium influx in *M. paleacea* control (AEQ-cas9) or single *lysm-rlk* mutants (as indicated) in response to 1mM hydrogen peroxide in water. Each trace represents the mean (line) ± standard deviation (shading) from three replicates over a time course of 15 min.

(**B**) Bar graph representation of the areas under the curves (A.U.C.) shown in (A). ANOVA revealed no statistical differences between mutants and control.

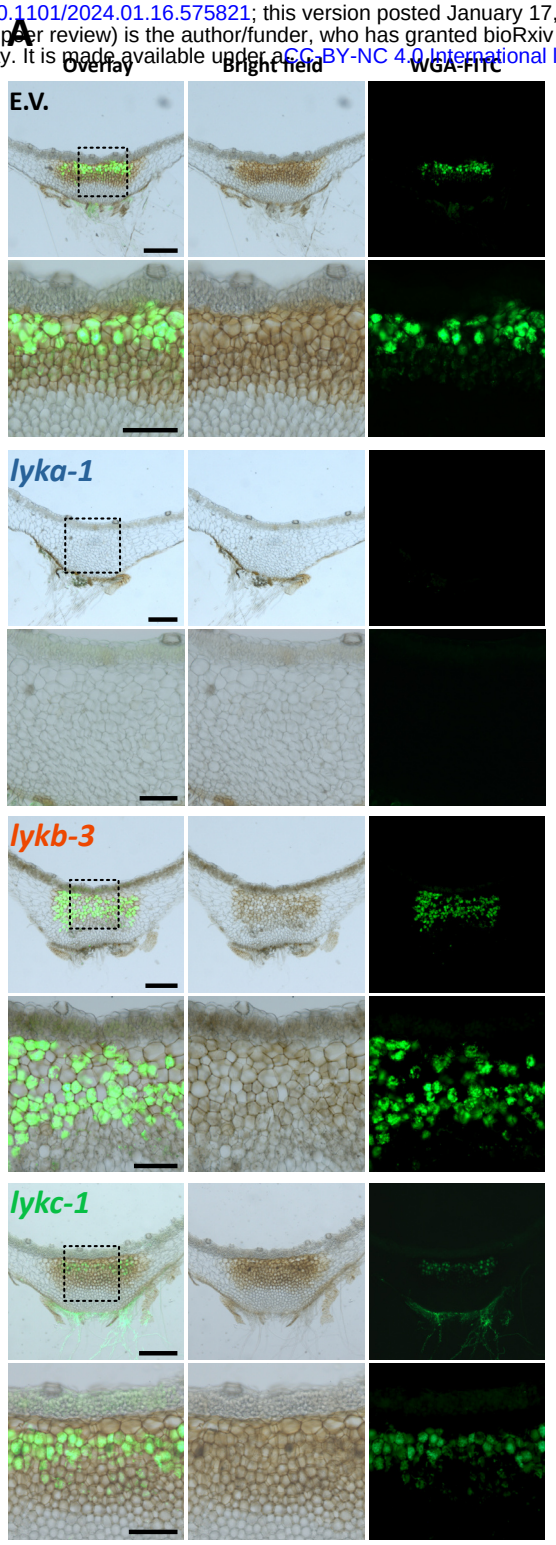

Figure 1.

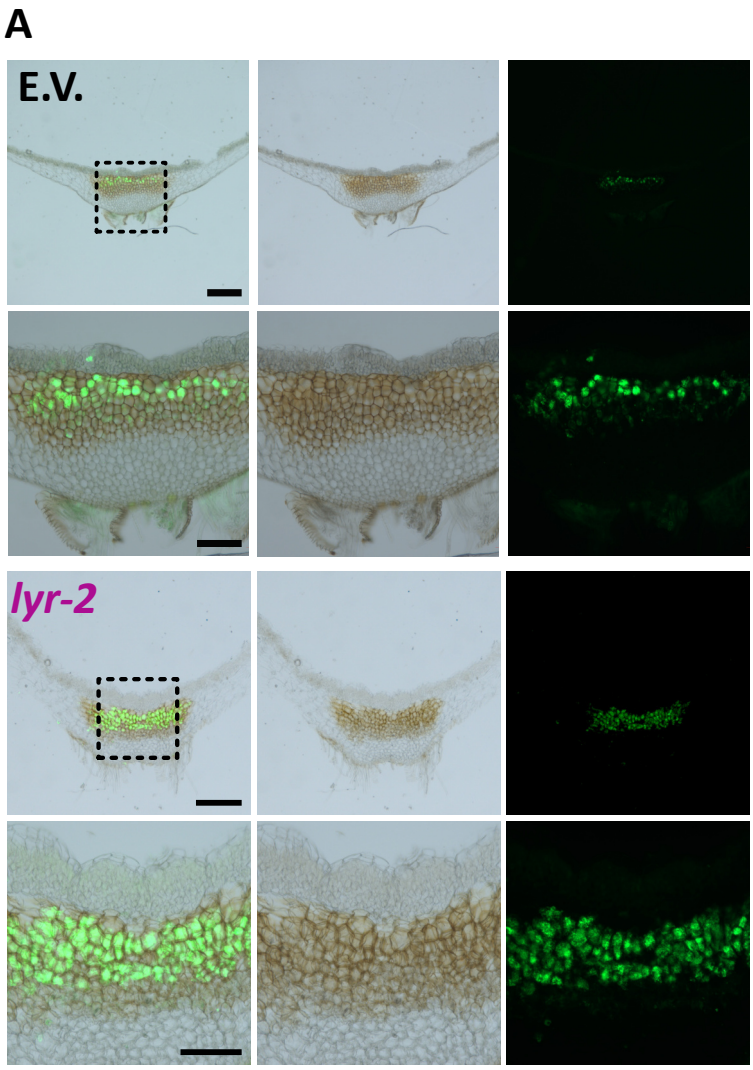

Figure 2.

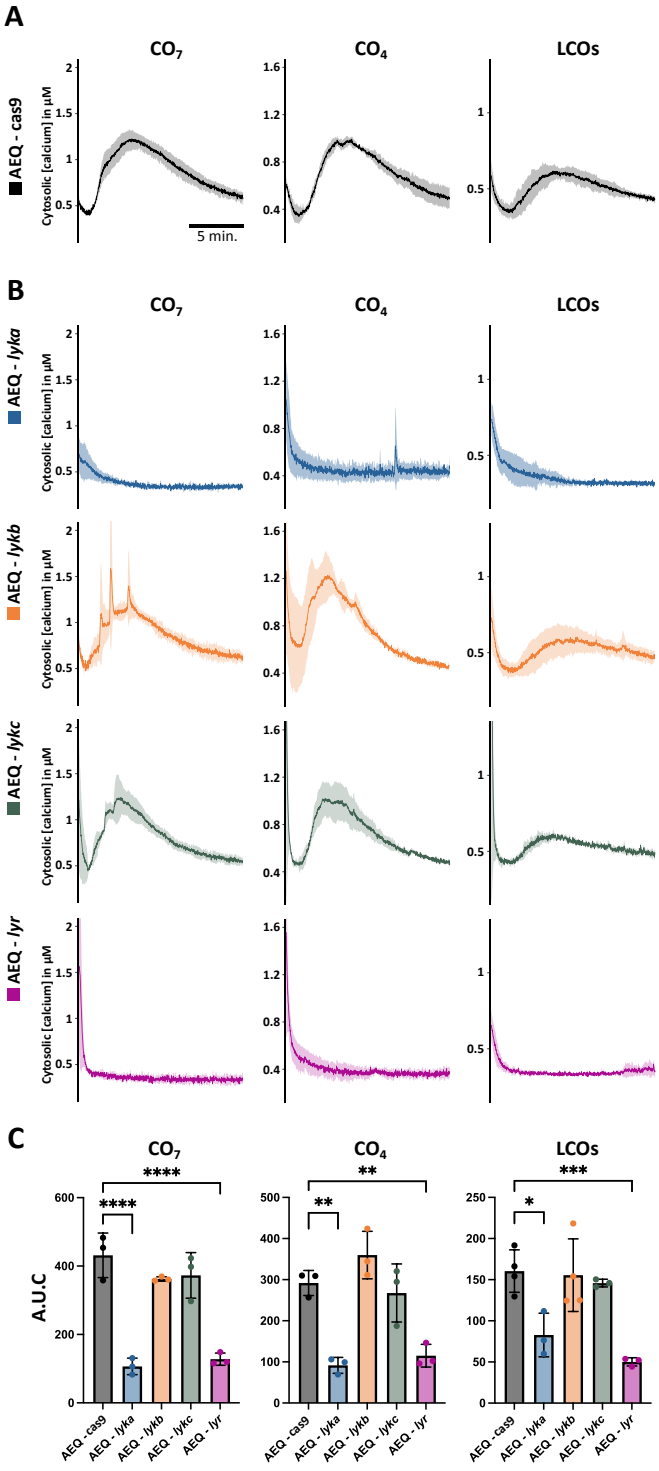

Figure 3.

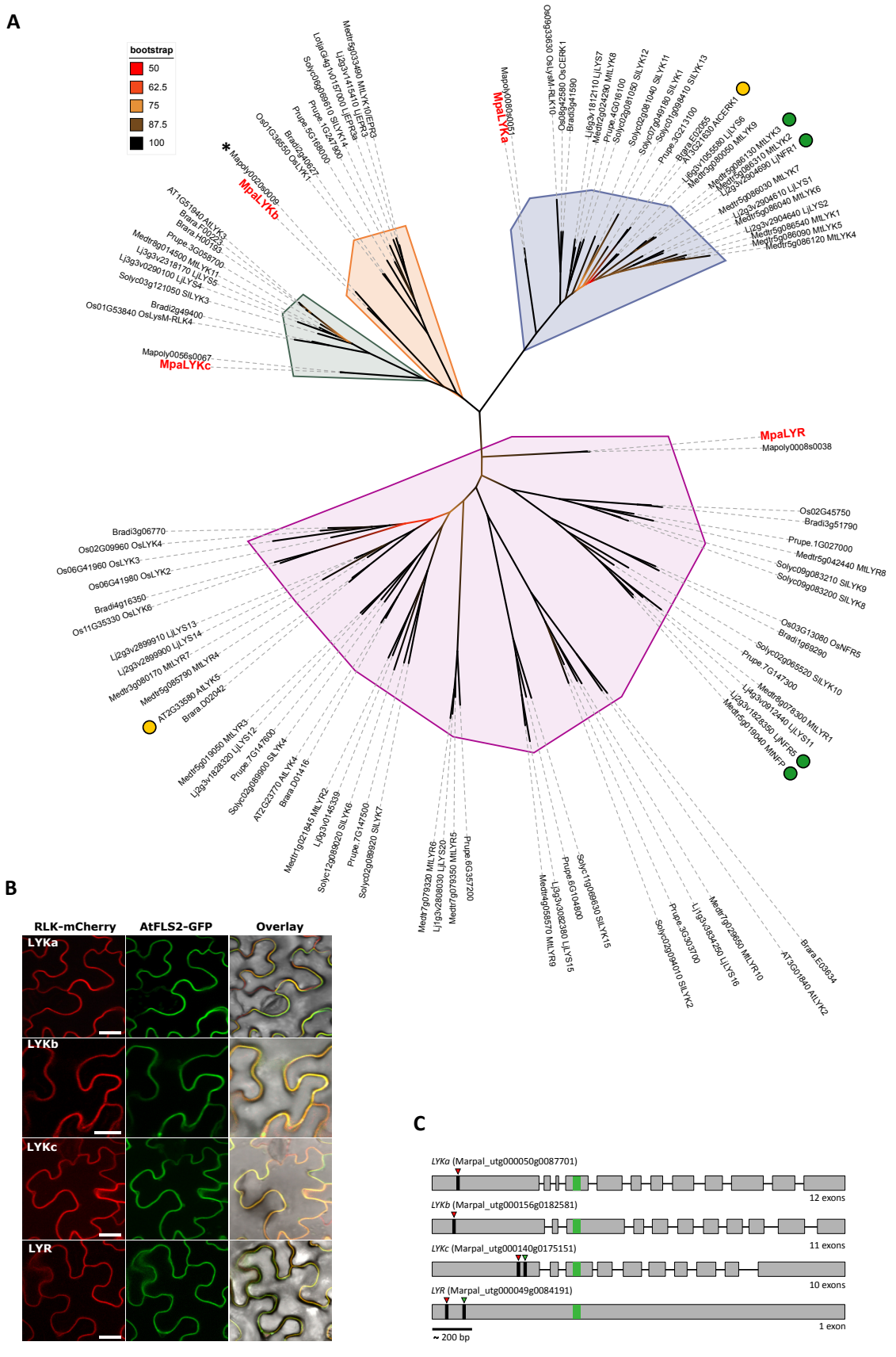

Supplementary Figure 1.

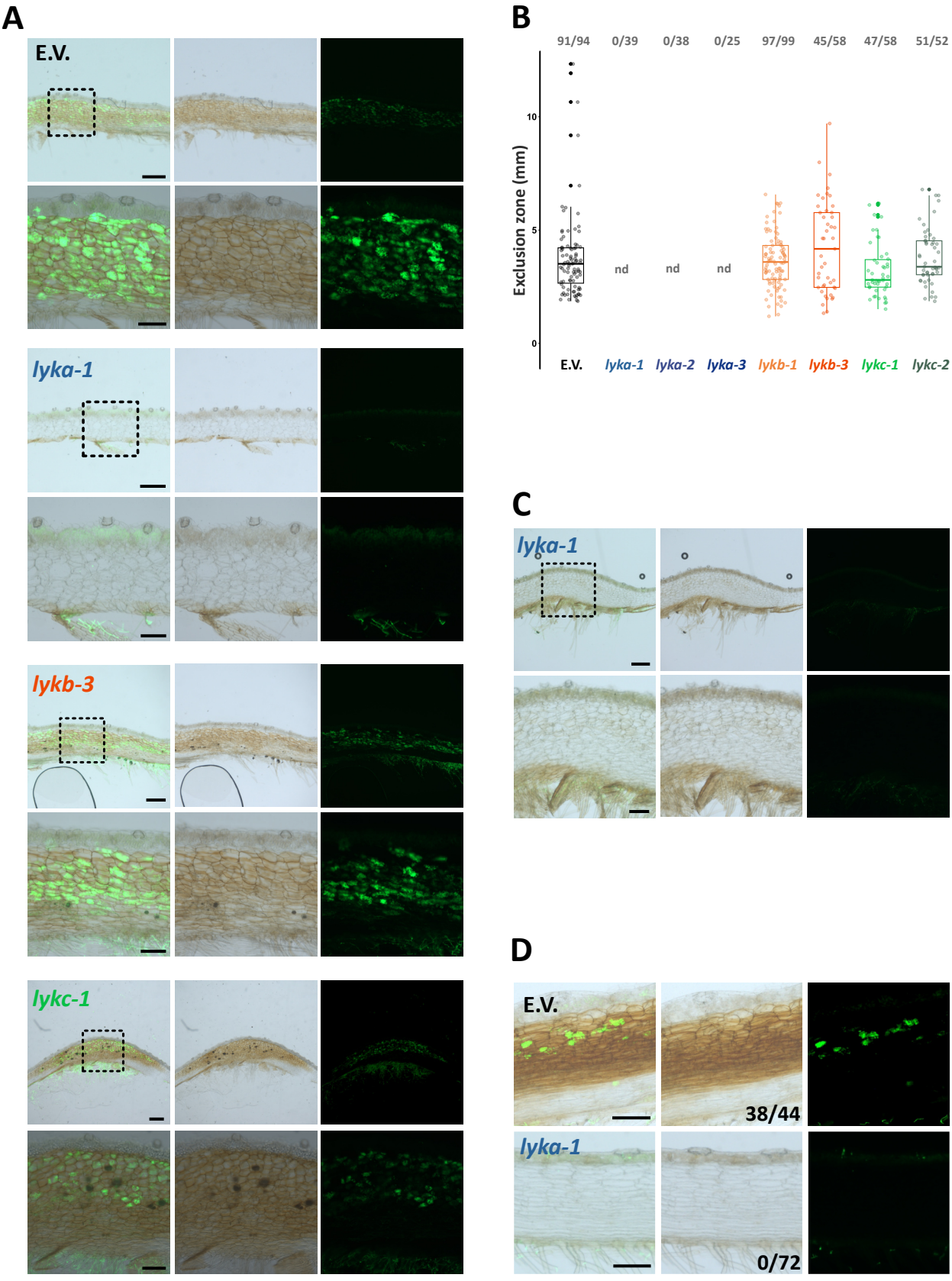

Supplementary Figure 2.

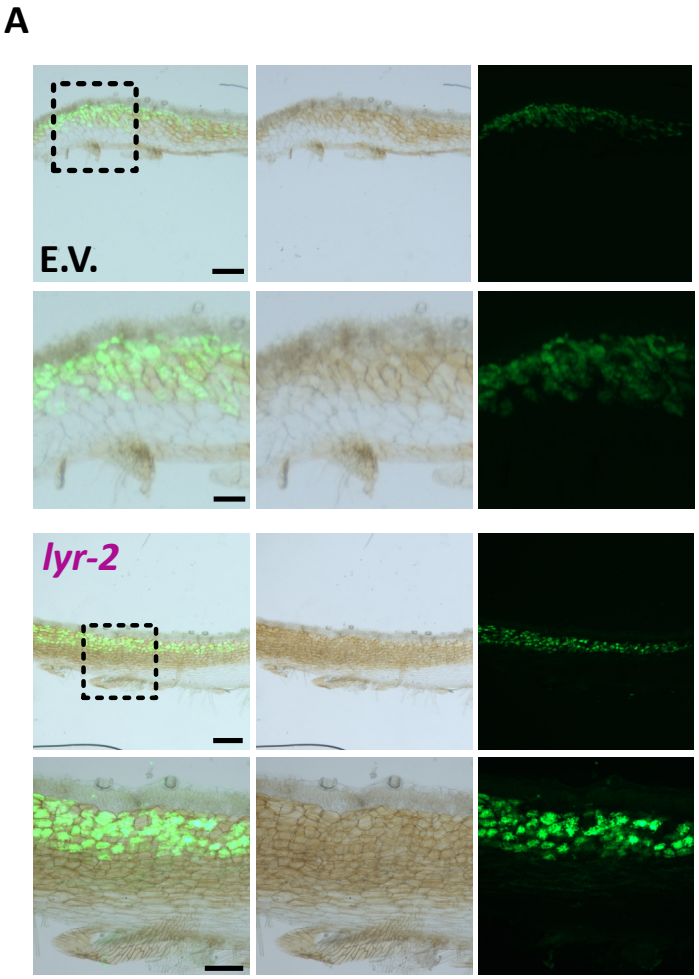

Supplementary Figure 3.

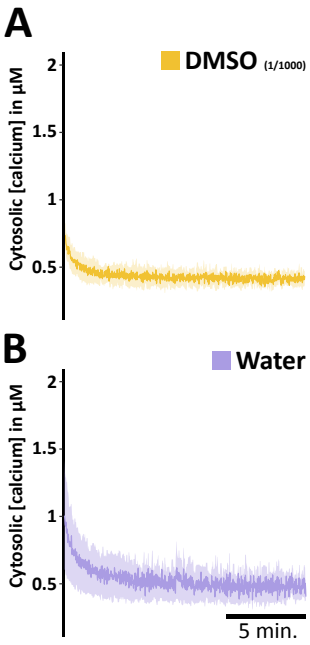

Supplementary Figure 4.

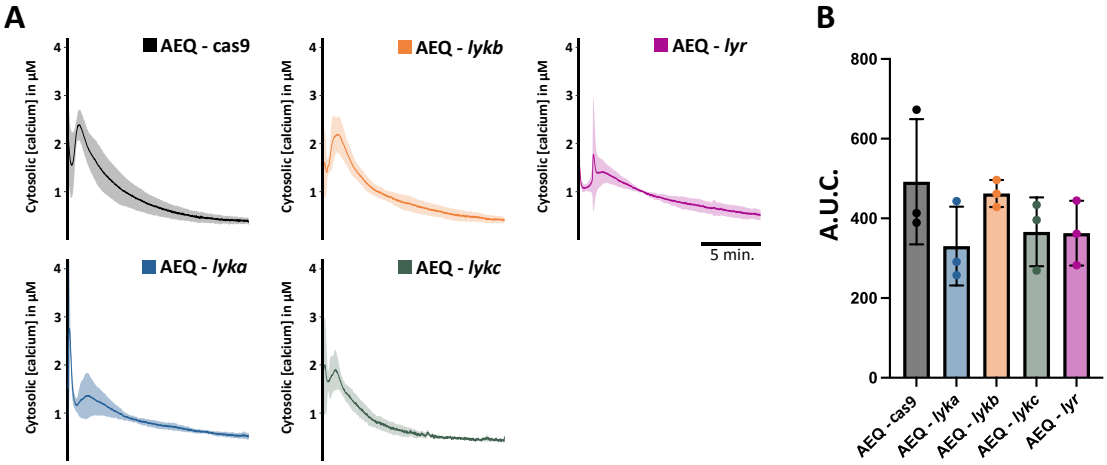

Supplementary Figure 5.

	Gene codes	Guide RNA code	Sequence	Mutant / Target name	Mutation
Guides sequences (w/o PAM)	Marpal_utg000050g0087701	gRNA #1		*lyka-1*	A insertion/frameshift at AA59 leading to STOP
		gRNA #1	TGATACTCTCCTAGCTCTGG	*lyka-2*	A insertion/frameshift at AA59 leading to STOP
		gRNA #1		*lyka-3*	A insertion/frameshift at AA59 leading to STOP
	Marpal_utg000156g0182581	gRNA #1		*lykb-1*	T insertion/frameshift AA29 leading to STOP
		gRNA #1	CGGAGCGGATTAATCAACTG	*lykb-2*	TT insertion/frameshift AA29 leading to STOP
		gRNA #1		*lykb-3*	19bp deletion/frameshit AA29 leading to STOP
	Marpal_utg000140g0175151	gRNA #1	GGACCGTTACGATGCGGATA	*lykc-1*	T insertion/frameshift at AA179 leading to STOP
		gRNA #2	GCTCGGGAAGTAGCTGACAT	*lykc-2*	G insertion/frameshift at AA192 leading to STOP
	Marpal_utg000049g0084191	gRNA #1	ACTCGTGCTCAACAGGTCTA	*lyr-1*	T insertion/frameshift at AA26 leading to STOP
		gRNA #2	TTACAAAGACATTCCCGCTG	*lyr-2*	A insertion/frameshift at AA61 leading to STOP
CRISPR guides	Marpal_utg000050g0087701	gRNA #1	TGATACTCTCCTAGCTCTGG	*AEQ-lyka*	1bp deletion/frameshit AA57 leading to STOP
	Marpal_utg000156g0182581	gRNA #1	CGGAGCGGATTAATCAACTG	*AEQ-lykb*	T insertion/frameshift at AA27 leading to STOP
	Marpal_utg000140g0175151	gRNA #1	GGACCGTTACGATGCGGATA	*AEQ-lykc*	G insertion/frameshift at AA179 leading to STOP
	Marpal_utg000049g0084191	gRNA #1	ACTCGTGCTCAACAGGTCTA	*AEQ-lyr*	T insertion/frameshift at AA26 leading to STOP
Primers for gRNA cloning	Marpal_utg000050g0087701_ g1	Forward	TCTCGTGATACTCTCCTAGCTCTGG	LYKa	
		Reverse	AAACCCAGAGCTAGGAGAGTATCAC		
	Marpal_utg000156g0182581_g1	Forward	TCTCGCGGAGCGGATTAATCAACTG	LYKb	
		Reverse	AAACCAGTTGATTAATCCGCTCCGC		
	Marpal_utg000140g0175151_g1	Forward	TCTCGGGACCGTTACGATGCGGATA	LYKc	
		Reverse	AAACTATCCGCATCGTAACGGTCCC		
	Marpal_utg000140g0175151_g2	Forward	TCTCGGCTCGGGAAGTAGCTGACAT	LYKc	
		Reverse	AAACATGTCAGCTACTTCCCGAGCC		
	Marpal_utg000049g0084191_g1	Forward	TCTCGACTCGTGCTCAACAGGTCTA	LYR	
		Reverse	AAACTAGACCTGTTGAGCACGAGTC		
	Marpal_utg000049g0084191_g2	Forward	TCTCGTTACAAAGACATTCCCGCTG	LYR	
		Reverse	AAACCAGCGGGAATGTCTTTGTAAC		
Genotyping primers	Marpal_utg000050g0087701	Forward	TGAGAATTCGCCTGTAGTTTG	LYKa	
		Reverse	ACCTTTCTGGGGGATAAAGATGA		
	Marpal_utg000156g0182581	Forward	ATGAGAGCGAGGAGTCCCGTA	LYKb	
		Reverse	GAAGTTGAGCGGGATGAAGAGGT		
	Marpal_utg000140g0175151	Forward	GTTTCAGACATCATGGAACAAAAAG	LYKc	
		Reverse	CCGTTCAACCGATCATAGTAC		
	Marpal_utg000049g0084191	Forward	AGGTGATTTCAAAGTGGGAGAC	LYR	
		Reverse	TCCAGAGTGTTGTTGCTGAG		

Supplementary Table 1.
List of primers used.